



## Improved Measurement of Mixing-induced $CP$ Violation in the Neutral $B$ Meson System

K. Abe,<sup>8</sup> K. Abe,<sup>41</sup> T. Abe,<sup>42</sup> I. Adachi,<sup>8</sup> H. Aihara,<sup>43</sup> M. Akatsu,<sup>21</sup> Y. Asano,<sup>48</sup> T. Aso,<sup>47</sup>  
V. Aulchenko,<sup>2</sup> T. Aushev,<sup>12</sup> A. M. Bakich,<sup>38</sup> E. Banas,<sup>26</sup> A. Bay,<sup>17</sup> P. K. Behera,<sup>49</sup>  
I. Bizjak,<sup>13</sup> A. Bondar,<sup>2</sup> A. Bozek,<sup>26</sup> M. Bračko,<sup>19,13</sup> J. Brodzicka,<sup>26</sup> T. E. Browder,<sup>7</sup>  
B. C. K. Casey,<sup>7</sup> P. Chang,<sup>25</sup> Y. Chao,<sup>25</sup> K.-F. Chen,<sup>25</sup> B. G. Cheon,<sup>37</sup> R. Chistov,<sup>12</sup>  
Y. Choi,<sup>37</sup> Y. K. Choi,<sup>37</sup> M. Danilov,<sup>12</sup> L. Y. Dong,<sup>10</sup> A. Drutskoy,<sup>12</sup> S. Eidelman,<sup>2</sup>  
V. Eiges,<sup>12</sup> Y. Enari,<sup>21</sup> C. W. Everton,<sup>20</sup> F. Fang,<sup>7</sup> H. Fujii,<sup>8</sup> C. Fukunaga,<sup>45</sup> N. Gabyshev,<sup>8</sup>  
A. Garmash,<sup>2,8</sup> T. Gershon,<sup>8</sup> B. Golob,<sup>18,13</sup> K. Gotow,<sup>50</sup> R. Guo,<sup>23</sup> J. Haba,<sup>8</sup>  
K. Hanagaki,<sup>32</sup> F. Handa,<sup>42</sup> K. Hara,<sup>30</sup> T. Hara,<sup>30</sup> Y. Harada,<sup>28</sup> N. C. Hastings,<sup>20</sup>  
H. Hayashii,<sup>22</sup> M. Hazumi,<sup>8</sup> E. M. Heenan,<sup>20</sup> I. Higuchi,<sup>42</sup> T. Higuchi,<sup>8</sup> L. Hinz,<sup>17</sup>  
T. Hojo,<sup>30</sup> T. Hokuue,<sup>21</sup> Y. Hoshi,<sup>41</sup> W.-S. Hou,<sup>25</sup> H.-C. Huang,<sup>25</sup> T. Igaki,<sup>21</sup> Y. Igarashi,<sup>8</sup>  
T. Iijima,<sup>21</sup> K. Inami,<sup>21</sup> A. Ishikawa,<sup>21</sup> H. Ishino,<sup>44</sup> R. Itoh,<sup>8</sup> H. Iwasaki,<sup>8</sup> Y. Iwasaki,<sup>8</sup>  
H. K. Jang,<sup>36</sup> H. Kakuno,<sup>44</sup> J. Kaneko,<sup>44</sup> J. H. Kang,<sup>52</sup> J. S. Kang,<sup>14</sup> N. Katayama,<sup>8</sup>  
H. Kawai,<sup>3</sup> H. Kawai,<sup>43</sup> Y. Kawakami,<sup>21</sup> N. Kawamura,<sup>1</sup> T. Kawasaki,<sup>28</sup> H. Kichimi,<sup>8</sup>  
D. W. Kim,<sup>37</sup> Heejong Kim,<sup>52</sup> H. J. Kim,<sup>52</sup> H. O. Kim,<sup>37</sup> Hyunwoo Kim,<sup>14</sup> K. Kinoshita,<sup>5</sup>  
S. Kobayashi,<sup>34</sup> K. Korotushenko,<sup>32</sup> S. Korpar,<sup>19,13</sup> P. Krizan,<sup>18,13</sup> P. Krokovny,<sup>2</sup>  
S. Kumar,<sup>31</sup> A. Kuzmin,<sup>2</sup> Y.-J. Kwon,<sup>52</sup> J. S. Lange,<sup>6,33</sup> G. Leder,<sup>11</sup> S. H. Lee,<sup>36</sup> J. Li,<sup>35</sup>  
A. Limosani,<sup>20</sup> J. MacNaughton,<sup>11</sup> G. Majumder,<sup>39</sup> F. Mandl,<sup>11</sup> D. Marlow,<sup>32</sup>  
S. Matsumoto,<sup>4</sup> T. Matsumoto,<sup>45</sup> W. Mitaroff,<sup>11</sup> K. Miyabayashi,<sup>22</sup> Y. Miyabayashi,<sup>21</sup>  
H. Miyake,<sup>30</sup> G. R. Moloney,<sup>20</sup> T. Mori,<sup>4</sup> A. Murakami,<sup>34</sup> T. Nagamine,<sup>42</sup> Y. Nagasaka,<sup>9</sup>  
T. Nakadaira,<sup>43</sup> E. Nakano,<sup>29</sup> M. Nakao,<sup>8</sup> H. Nakazawa,<sup>4</sup> J. W. Nam,<sup>37</sup> Z. Natkaniec,<sup>26</sup>  
K. Neichi,<sup>41</sup> S. Nishida,<sup>15</sup> O. Nitoh,<sup>46</sup> S. Noguchi,<sup>22</sup> T. Nozaki,<sup>8</sup> S. Ogawa,<sup>40</sup> T. Ohshima,<sup>21</sup>  
T. Okabe,<sup>21</sup> S. L. Olsen,<sup>7</sup> Y. Onuki,<sup>28</sup> W. Ostrowicz,<sup>26</sup> H. Ozaki,<sup>8</sup> P. Pakhlov,<sup>12</sup>  
H. Palka,<sup>26</sup> C. W. Park,<sup>14</sup> H. Park,<sup>16</sup> K. S. Park,<sup>37</sup> J.-P. Perroud,<sup>17</sup> L. E. Pilonen,<sup>50</sup>  
F. J. Ronga,<sup>17</sup> N. Root,<sup>2</sup> M. Rozanska,<sup>26</sup> K. Rybicki,<sup>26</sup> H. Sagawa,<sup>8</sup> S. Saitoh,<sup>8</sup> Y. Sakai,<sup>8</sup>  
H. Sakamoto,<sup>15</sup> M. Satapathy,<sup>49</sup> A. Satpathy,<sup>8,5</sup> O. Schneider,<sup>17</sup> S. Schrenk,<sup>5</sup>  
C. Schwanda,<sup>8,11</sup> S. Semenov,<sup>12</sup> K. Senyo,<sup>21</sup> R. Seuster,<sup>7</sup> H. Shibuya,<sup>40</sup> B. Shwartz,<sup>2</sup>  
V. Sidorov,<sup>2</sup> J. B. Singh,<sup>31</sup> N. Soni,<sup>31</sup> S. Stanič,<sup>48,\*</sup> A. Sugi,<sup>21</sup> A. Sugiyama,<sup>21</sup>  
K. Sumisawa,<sup>8</sup> T. Sumiyoshi,<sup>45</sup> K. Suzuki,<sup>8</sup> S. Suzuki,<sup>51</sup> S. Y. Suzuki,<sup>8</sup> H. Tajima,<sup>43</sup>  
T. Takahashi,<sup>29</sup> F. Takasaki,<sup>8</sup> K. Tamai,<sup>8</sup> N. Tamura,<sup>28</sup> J. Tanaka,<sup>43</sup> M. Tanaka,<sup>8</sup>  
G. N. Taylor,<sup>20</sup> Y. Teramoto,<sup>29</sup> S. Tokuda,<sup>21</sup> T. Tomura,<sup>43</sup> K. Trabelsi,<sup>7</sup> W. Trischuk,<sup>32,†</sup>  
T. Tsuboyama,<sup>8</sup> T. Tsukamoto,<sup>8</sup> S. Uehara,<sup>8</sup> K. Ueno,<sup>25</sup> Y. Unno,<sup>3</sup> S. Uno,<sup>8</sup>  
N. Uozaki,<sup>43</sup> Y. Ushiroda,<sup>8</sup> S. E. Vahsen,<sup>32</sup> G. Varner,<sup>7</sup> K. E. Varvell,<sup>38</sup> C. C. Wang,<sup>25</sup>  
C. H. Wang,<sup>24</sup> J. G. Wang,<sup>50</sup> M.-Z. Wang,<sup>25</sup> Y. Watanabe,<sup>44</sup> E. Won,<sup>14</sup> B. D. Yabsley,<sup>50</sup>  
Y. Yamada,<sup>8</sup> A. Yamaguchi,<sup>42</sup> H. Yamamoto,<sup>42</sup> Y. Yamashita,<sup>43</sup> Y. Yamashita,<sup>27</sup>  
M. Yamauchi,<sup>8</sup> H. Yanai,<sup>28</sup> J. Yashima,<sup>8</sup> P. Yeh,<sup>25</sup> M. Yokoyama,<sup>43</sup> Y. Yuan,<sup>10</sup> Y. Yusa,<sup>42</sup>  
H. Yuta,<sup>1</sup> C. C. Zhang,<sup>10</sup> J. Zhang,<sup>48</sup> Z. P. Zhang,<sup>35</sup> V. Zhilich,<sup>2</sup> and D. Žontar<sup>48</sup>

(The Belle Collaboration)

- <sup>1</sup>*Aomori University, Aomori*
- <sup>2</sup>*Budker Institute of Nuclear Physics, Novosibirsk*
- <sup>3</sup>*Chiba University, Chiba*
- <sup>4</sup>*Chuo University, Tokyo*
- <sup>5</sup>*University of Cincinnati, Cincinnati OH*
- <sup>6</sup>*University of Frankfurt, Frankfurt*
- <sup>7</sup>*University of Hawaii, Honolulu HI*
- <sup>8</sup>*High Energy Accelerator Research Organization (KEK), Tsukuba*
- <sup>9</sup>*Hiroshima Institute of Technology, Hiroshima*
- <sup>10</sup>*Institute of High Energy Physics, Chinese Academy of Sciences, Beijing*
- <sup>11</sup>*Institute of High Energy Physics, Vienna*
- <sup>12</sup>*Institute for Theoretical and Experimental Physics, Moscow*
- <sup>13</sup>*J. Stefan Institute, Ljubljana*
- <sup>14</sup>*Korea University, Seoul*
- <sup>15</sup>*Kyoto University, Kyoto*
- <sup>16</sup>*Kyungpook National University, Taegu*
- <sup>17</sup>*Institut de Physique des Hautes Énergies, Université de Lausanne, Lausanne*
- <sup>18</sup>*University of Ljubljana, Ljubljana*
- <sup>19</sup>*University of Maribor, Maribor*
- <sup>20</sup>*University of Melbourne, Victoria*
- <sup>21</sup>*Nagoya University, Nagoya*
- <sup>22</sup>*Nara Women's University, Nara*
- <sup>23</sup>*National Kaohsiung Normal University, Kaohsiung*
- <sup>24</sup>*National Lien-Ho Institute of Technology, Miao Li*
- <sup>25</sup>*National Taiwan University, Taipei*
- <sup>26</sup>*H. Niewodniczanski Institute of Nuclear Physics, Krakow*
- <sup>27</sup>*Nihon Dental College, Niigata*
- <sup>28</sup>*Niigata University, Niigata*
- <sup>29</sup>*Osaka City University, Osaka*
- <sup>30</sup>*Osaka University, Osaka*
- <sup>31</sup>*Panjab University, Chandigarh*
- <sup>32</sup>*Princeton University, Princeton NJ*
- <sup>33</sup>*RIKEN BNL Research Center, Brookhaven NY*
- <sup>34</sup>*Saga University, Saga*
- <sup>35</sup>*University of Science and Technology of China, Hefei*
- <sup>36</sup>*Seoul National University, Seoul*
- <sup>37</sup>*Sungkyunkwan University, Suwon*
- <sup>38</sup>*University of Sydney, Sydney NSW*
- <sup>39</sup>*Tata Institute of Fundamental Research, Bombay*
- <sup>40</sup>*Toho University, Funabashi*
- <sup>41</sup>*Tohoku Gakuin University, Tagajo*
- <sup>42</sup>*Tohoku University, Sendai*
- <sup>43</sup>*University of Tokyo, Tokyo*
- <sup>44</sup>*Tokyo Institute of Technology, Tokyo*
- <sup>45</sup>*Tokyo Metropolitan University, Tokyo*

<sup>46</sup>*Tokyo University of Agriculture and Technology, Tokyo*  
<sup>47</sup>*Toyama National College of Maritime Technology, Toyama*

<sup>48</sup>*University of Tsukuba, Tsukuba*

<sup>49</sup>*Utkal University, Bhubaneswer*

<sup>50</sup>*Virginia Polytechnic Institute and State University, Blacksburg VA*

<sup>51</sup>*Yokkaichi University, Yokkaichi*

<sup>52</sup>*Yonsei University, Seoul*

(Dated: November 3, 2018)

## Abstract

We present an improved measurement of the standard model  $CP$  violation parameter  $\sin 2\phi_1$  (also known as  $\sin 2\beta$ ) based on a sample of  $85 \times 10^6$   $B\bar{B}$  pairs collected at the  $\Upsilon(4S)$  resonance with the Belle detector at the KEKB asymmetric-energy  $e^+e^-$  collider. One neutral  $B$  meson is reconstructed in a  $J/\psi K_S^0$ ,  $\psi(2S)K_S^0$ ,  $\chi_{c1}K_S^0$ ,  $\eta_c K_S^0$ ,  $J/\psi K^{*0}$ , or  $J/\psi K_L^0$   $CP$ -eigenstate decay channel and the flavor of the accompanying  $B$  meson is identified from its decay products. From the asymmetry in the distribution of the time interval between the two  $B$  meson decay points, we obtain  $\sin 2\phi_1 = 0.719 \pm 0.074(\text{stat}) \pm 0.035(\text{syst})$ .

PACS numbers: 11.30.Er, 12.15.Hh, 13.25.Hw

In the standard model (SM),  $CP$  violation arises from an irreducible complex phase in the weak interaction quark-mixing matrix [Cabibbo-Kobayashi-Maskawa (CKM) matrix] [1]. In particular, the SM predicts a  $CP$ -violating asymmetry in the time-dependent rates for  $B^0$  and  $\bar{B}^0$  decays to a common  $CP$  eigenstate  $f_{CP}$ , where the transition is dominated by the  $b \rightarrow c\bar{c}s$  process, with negligible corrections from strong interactions [2]:

$$A(t) \equiv \frac{\Gamma(\bar{B}^0 \rightarrow f_{CP}) - \Gamma(B^0 \rightarrow f_{CP})}{\Gamma(\bar{B}^0 \rightarrow f_{CP}) + \Gamma(B^0 \rightarrow f_{CP})} = -\xi_f \sin 2\phi_1 \sin(\Delta m_d t), \quad (1)$$

where  $\Gamma(B^0, \bar{B}^0 \rightarrow f_{CP})$  is the rate for  $B^0$  or  $\bar{B}^0$  to  $f_{CP}$  at a proper time  $t$  after production,  $\xi_f$  is the  $CP$  eigenvalue of  $f_{CP}$ ,  $\Delta m_d$  is the mass difference between the two  $B^0$  mass eigenstates, and  $\phi_1$  is one of the three interior angles of the CKM unitarity triangle, defined as  $\phi_1 \equiv \pi - \arg(V_{tb}^* V_{td} / V_{cb}^* V_{cd})$ . Non-zero values for  $\sin 2\phi_1$  have been reported by the Belle and BaBar groups [3, 4].

Belle's published measurement of  $\sin 2\phi_1$  is based on a  $29.1 \text{ fb}^{-1}$  data sample containing  $31.3 \times 10^6 B\bar{B}$  pairs produced at the  $\Upsilon(4S)$  resonance. In this paper, we report an improved measurement that uses  $85 \times 10^6 B\bar{B}$  pairs ( $78 \text{ fb}^{-1}$ ). Two important changes exist in the analysis with respect to the published result [3]; we apply a new track reconstruction algorithm that provides better performance and a new proper-time interval resolution function [5] that reduces systematic uncertainties in  $\sin 2\phi_1$ . The data were collected with the Belle detector [6] at the KEKB asymmetric collider [7], which collides  $8.0 \text{ GeV } e^-$  on  $3.5 \text{ GeV } e^+$  at a small ( $\pm 11 \text{ mrad}$ ) crossing angle. We use events where one of the  $B$  mesons decays to  $f_{CP}$  at time  $t_{CP}$ , and the other decays to a self-tagging state  $f_{\text{tag}}$ , which distinguishes  $B^0$  from  $\bar{B}^0$ , at time  $t_{\text{tag}}$ . The  $CP$  violation manifests itself as an asymmetry  $A(\Delta t)$ , where  $\Delta t$  is the proper time interval between the two decays:  $\Delta t \equiv t_{CP} - t_{\text{tag}}$ . At KEKB, the  $\Upsilon(4S)$  resonance is produced with a boost of  $\beta\gamma = 0.425$  nearly along the  $z$  axis defined as anti-parallel to the positron beam direction, and  $\Delta t$  can be determined as  $\Delta t \simeq \Delta z / (\beta\gamma)c$ , where  $\Delta z$  is the  $z$  distance between the  $f_{CP}$  and  $f_{\text{tag}}$  decay vertices,  $\Delta z \equiv z_{CP} - z_{\text{tag}}$ . The average value of  $\Delta z$  is approximately  $200 \mu\text{m}$ .

The Belle detector [6] is a large-solid-angle spectrometer that includes a silicon vertex detector (SVD), a central drift chamber (CDC), an array of aerogel threshold Čerenkov counters (ACC), time-of-flight (TOF) scintillation counters, and an electromagnetic calorimeter comprised of CsI(Tl) crystals (ECL) located inside a superconducting solenoid coil that provides a  $1.5 \text{ T}$  magnetic field. An iron flux-return located outside of the coil is instrumented to detect  $K_L^0$  mesons and to identify muons (KLM).

We reconstruct  $B^0$  decays to the following  $CP$  eigenstates [8]:  $J/\psi K_S^0$ ,  $\psi(2S)K_S^0$ ,  $\chi_{c1}K_S^0$ ,  $\eta_c K_S^0$  for  $\xi_f = -1$  and  $J/\psi K_L^0$  for  $\xi_f = +1$ . We also use  $B^0 \rightarrow J/\psi K^{*0}$  decays where  $K^{*0} \rightarrow K_S^0 \pi^0$ . Here the final state is a mixture of even and odd  $CP$ , depending on the relative orbital angular momentum of the  $J/\psi$  and  $K^{*0}$ . We find that the final state is primarily  $\xi_f = +1$ ; the  $\xi_f = -1$  fraction is  $0.19 \pm 0.02(\text{stat}) \pm 0.03(\text{syst})$  [9].  $J/\psi$  and  $\psi(2S)$  mesons are reconstructed via their decays to  $\ell^+ \ell^-$  ( $\ell = \mu, e$ ). The  $\psi(2S)$  is also reconstructed via  $J/\psi \pi^+ \pi^-$ , and the  $\chi_{c1}$  via  $J/\psi \gamma$ . The  $\eta_c$  is detected in the  $K_S^0 K^- \pi^+$ ,  $K^+ K^- \pi^0$ , and  $p\bar{p}$  modes. For the  $J/\psi K_S^0$  mode, we use  $K_S^0 \rightarrow \pi^+ \pi^-$  and  $\pi^0 \pi^0$  decays; for other modes we only use  $K_S^0 \rightarrow \pi^+ \pi^-$ . For reconstructed  $B \rightarrow f_{CP}$  candidates other than  $J/\psi K_L^0$ , we identify  $B$  decays using the energy difference  $\Delta E \equiv E_B^{\text{cms}} - E_{\text{beam}}^{\text{cms}}$  and the beam-energy constrained mass  $M_{\text{bc}} \equiv \sqrt{(E_{\text{beam}}^{\text{cms}})^2 - (p_B^{\text{cms}})^2}$ , where  $E_{\text{beam}}^{\text{cms}}$  is the beam energy in the center-of-mass system (cms) of the  $\Upsilon(4S)$  resonance, and  $E_B^{\text{cms}}$  and  $p_B^{\text{cms}}$  are the cms energy and momentum of the reconstructed  $B$  candidate, respectively. Figure 1

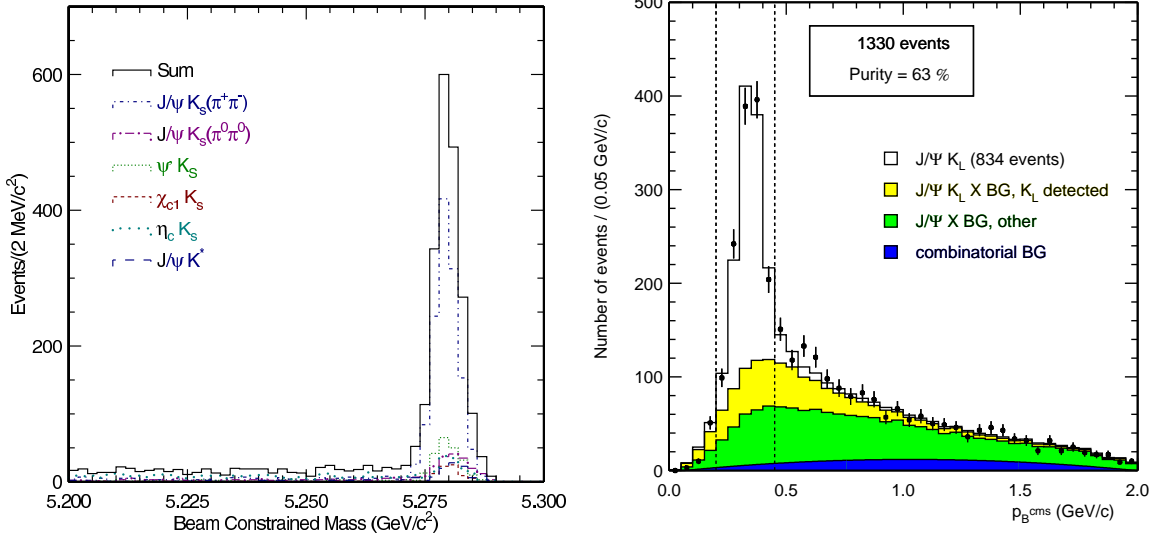


FIG. 1: The beam-energy constrained mass distribution for all decay modes other than  $J/\psi K_L^0$  (left). The  $p_B^{\text{cms}}$  distribution for  $B^0 \rightarrow J/\psi K_L^0$  candidates with the results of the fit (right).

TABLE I: The numbers of reconstructed  $B \rightarrow f_{CP}$  candidates before flavor tagging and vertex reconstruction,  $N_{\text{rec}}$ , the numbers of events used for the  $\sin 2\phi_1$  determination,  $N_{\text{ev}}$ , and the estimated signal purity in the signal region for each  $f_{CP}$  mode.

Mode	$\xi_f$	$N_{\text{rec}}$	$N_{\text{ev}}$	Purity
$J/\psi(\ell^+\ell^-)K_S^0(\pi^+\pi^-)$	-1	1285	1116	$0.976 \pm 0.001$
$J/\psi(\ell^+\ell^-)K_S^0(\pi^0\pi^0)$	-1	188	162	$0.82 \pm 0.02$
$\psi(2S)(\ell^+\ell^-)K_S^0(\pi^+\pi^-)$	-1	91	76	$0.96 \pm 0.01$
$\psi(2S)(J/\psi\pi^+\pi^-)K_S^0(\pi^+\pi^-)$	-1	112	96	$0.91 \pm 0.01$
$\chi_{c1}(J/\psi\gamma)K_S^0(\pi^+\pi^-)$	-1	77	67	$0.96 \pm 0.01$
$\eta_c(K_S^0 K^- \pi^+)K_S^0(\pi^+\pi^-)$	-1	72	63	$0.65 \pm 0.04$
$\eta_c(K^+ K^- \pi^0)K_S^0(\pi^+\pi^-)$	-1	49	44	$0.72 \pm 0.04$
$\eta_c(p\bar{p})K_S^0(\pi^+\pi^-)$	-1	21	15	$0.94 \pm 0.02$
All with $\xi_f = -1$	-1	1895	1639	$0.936 \pm 0.003$
$J/\psi(\ell^+\ell^-)K^{*0}(K_S^0\pi^0)$	-1(19%)/+1(81%)	101	89	$0.92 \pm 0.01$
$J/\psi(\ell^+\ell^-)K_L^0$	+1	1330	1230	$0.63 \pm 0.04$
All		3326	2958	$0.81 \pm 0.01$

(left) shows the  $M_{bc}$  distributions for all  $B^0$  candidates except for  $B^0 \rightarrow J/\psi K_L^0$  that have  $\Delta E$  values in the signal region. Table I lists the numbers of observed candidates,  $N_{\text{rec}}$ .

Candidate  $B^0 \rightarrow J/\psi K_L^0$  decays are selected by requiring ECL and/or KLM hit patterns that are consistent with the presence of a shower induced by a  $K_L^0$  meson. The centroid of the shower is required to be within a  $45^\circ$  cone centered on the  $K_L^0$  direction inferred from two-body decay kinematics and the measured four-momentum of the  $J/\psi$ . Figure 1 (right)

TABLE II: The event fractions  $\epsilon_l$ , wrong tag fractions  $w_l$ , and effective tagging efficiencies  $\epsilon_{\text{eff}}^l = \epsilon_l(1 - 2w_l)^2$  for each  $r$  interval. The errors include both statistical and systematic uncertainties. The event fractions are obtained from the  $J/\psi K_S^0$  simulation.

$l$	$r$ interval	$\epsilon_l$	$w_l$	$\epsilon_{\text{eff}}^l$
1	0.000 – 0.250	0.398	$0.458 \pm 0.006$	$0.003 \pm 0.001$
2	0.250 – 0.500	0.146	$0.336 \pm 0.009$	$0.016 \pm 0.002$
3	0.500 – 0.625	0.104	$0.228 \pm 0.010$	$0.031 \pm 0.002$
4	0.625 – 0.750	0.122	$0.160^{+0.009}_{-0.008}$	$0.056 \pm 0.003$
5	0.750 – 0.875	0.094	$0.112 \pm 0.009$	$0.056 \pm 0.003$
6	0.875 – 1.000	0.136	$0.020 \pm 0.006$	$0.126^{+0.003}_{-0.004}$

shows the  $p_B^{\text{cms}}$  distribution, calculated with the  $B^0 \rightarrow J/\psi K_L^0$  two-body decay hypothesis. The histograms are the results of a fit to the signal and background distributions. There are 1330 entries in total in the  $0.20 \leq p_B^{\text{cms}} \leq 0.45$  GeV/ $c$  signal region; the fit indicates a signal purity of 63%. The reconstruction and selection criteria for all  $f_{CP}$  channels used in the measurement are described in more detail elsewhere [3].

Charged leptons, pions, kaons, and  $\Lambda$  baryons that are not associated with a reconstructed  $CP$  eigenstate decay are used to identify the  $b$ -flavor of the accompanying  $B$  meson. Based on the measured properties of these tracks, two parameters,  $q$  and  $r$ , are assigned to an event. The first,  $q$ , has the discrete value  $+1$  ( $-1$ ) when the tag-side  $B$  meson is likely to be a  $B^0$  ( $\bar{B}^0$ ), and the parameter  $r$  is an event-by-event Monte-Carlo-determined flavor-tagging dilution factor that ranges from  $r = 0$  for no flavor discrimination to  $r = 1$  for an unambiguous flavor assignment. It is used only to sort data into six intervals of  $r$ , according to estimated flavor purity. The wrong-tag probabilities,  $w_l$  ( $l = 1, 6$ ), that are used in the final fit are determined directly from data. Samples of  $B^0$  decays to exclusively reconstructed self-tagging channels are utilized to obtain  $w_l$  using time-dependent  $B^0$ - $\bar{B}^0$  mixing oscillation:  $(N_{\text{OF}} - N_{\text{SF}})/(N_{\text{OF}} + N_{\text{SF}}) = (1 - 2w_l) \cos(\Delta m_d \Delta t)$ , where  $N_{\text{OF}}$  and  $N_{\text{SF}}$  are the numbers of opposite and same flavor events. The event fractions and wrong tag fractions are summarized in Table II. The total effective tagging efficiency is determined to be  $\epsilon_{\text{eff}} \equiv \sum_{l=1}^6 \epsilon_l(1 - 2w_l)^2 = 0.288 \pm 0.006$ , where  $\epsilon_l$  is the event fraction for each  $r$  interval. The error includes both statistical and systematic uncertainties. Improvements in the Monte Carlo simulation [10] and in the track reconstruction yield  $\epsilon_{\text{eff}}$  that is higher by 6.7% (relative) than the value in Ref. [3].

The vertex position for the  $f_{CP}$  decay is reconstructed using leptons from  $J/\psi$  decays or charged hadrons from  $\eta_c$  decays, and that for  $f_{\text{tag}}$  is obtained with well reconstructed tracks that are not assigned to  $f_{CP}$ . Tracks that are consistent with coming from a  $K_S^0 \rightarrow \pi^+\pi^-$  decay are not used. Each vertex position is required to be consistent with the interaction region profile, determined run-by-run, smeared in the  $r$ - $\phi$  plane to account for the  $B$  meson decay length. With these requirements, we are able to determine a vertex even with a single track; the fraction of single-track vertices is about 10% for  $z_{CP}$  and 22% for  $z_{\text{tag}}$ . The proper-time interval resolution function  $R_{\text{sig}}(\Delta t)$  is formed by convolving four components: the detector resolutions for  $z_{CP}$  and  $z_{\text{tag}}$ , the shift in the  $z_{\text{tag}}$  vertex position due to secondary tracks originating from charmed particle decays, and the kinematic approximation that the  $B$  mesons are at rest in the cms [5]. A small component of broad outliers in the  $\Delta z$  distribution, caused by mis-reconstruction, is represented by a Gaussian function. We determine twelve

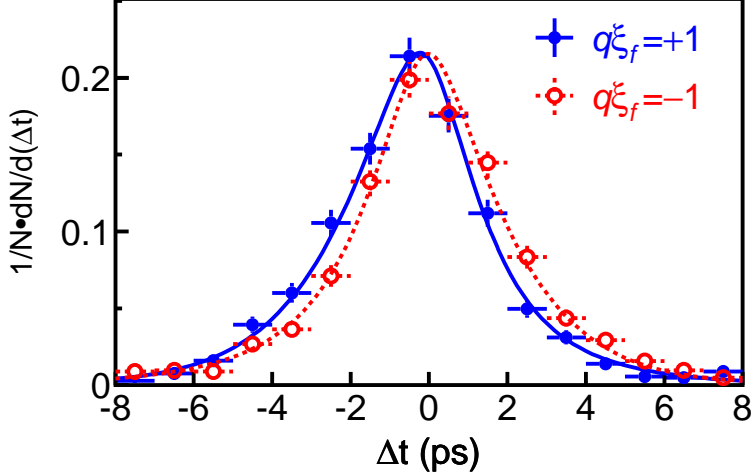


FIG. 2: The  $\Delta t$  distributions for the events with  $q\xi_f = +1$  (solid points) and  $q\xi_f = -1$  (open points). The results of the global fit with  $\sin 2\phi_1 = 0.719$  are shown as solid and dashed curves, respectively.

resolution parameters from fits of data to the neutral and charged  $B$  meson lifetimes [5] and obtain an average  $\Delta t$  resolution of  $\sim 1.43$  ps (rms). The width of the outlier component is determined to be  $42_{-4}^{+5}$  ps; the fractions of the outlier components are  $(2 \pm 1) \times 10^{-4}$  for events with both vertices reconstructed with more than one track, and  $(2.7 \pm 0.2) \times 10^{-2}$  for events with at least one single-track vertex.

After flavor tagging and vertexing, we find 1465 events with  $q = +1$  flavor tags and 1493 events with  $q = -1$ . Table I lists the numbers of candidates used for the  $\sin 2\phi_1$  determination,  $N_{ev}$ , and the estimated signal purity in the signal region for each  $f_{CP}$  mode. Figure 2 shows the observed  $\Delta t$  distributions for the  $q\xi_f = +1$  (solid points) and  $q\xi_f = -1$  (open points) event samples. The asymmetry between the two distributions demonstrates the violation of  $CP$  symmetry. We determine  $\sin 2\phi_1$  from an unbinned maximum-likelihood fit to the observed  $\Delta t$  distributions. The probability density function (PDF) expected for the signal distribution is given by

$$\mathcal{P}_{\text{sig}}(\Delta t, q, w_l, \xi_f) = \frac{e^{-|\Delta t|/\tau_{B^0}}}{4\tau_{B^0}} [1 - q\xi_f(1 - 2w_l)\sin 2\phi_1 \sin(\Delta m_d \Delta t)], \quad (2)$$

where we fix the  $B^0$  lifetime  $\tau_{B^0}$  and mass difference at their world average values [11]. Each PDF is convolved with the appropriate  $R_{\text{sig}}(\Delta t)$  to determine the likelihood value for each event as a function of  $\sin 2\phi_1$ :

$$P_i = (1 - f_{\text{ol}}) \int \left[ f_{\text{sig}} \mathcal{P}_{\text{sig}}(\Delta t', q, w_l, \xi_f) R_{\text{sig}}(\Delta t - \Delta t') + (1 - f_{\text{sig}}) \mathcal{P}_{\text{bkg}}(\Delta t') R_{\text{bkg}}(\Delta t - \Delta t') \right] d\Delta t' + f_{\text{ol}} P_{\text{ol}}(\Delta t), \quad (3)$$

where  $f_{\text{sig}}$  is the signal fraction calculated as a function of  $p_B^{\text{cms}}$  for  $J/\psi K_L^0$  and of  $\Delta E$  and  $M_{\text{bc}}$  for other modes.  $\mathcal{P}_{\text{bkg}}(\Delta t)$  is the PDF for combinatorial background events, which is modeled as a sum of exponential and prompt components. It is convolved with a sum of two Gaussians,  $R_{\text{bkg}}$ , which is regarded as a resolution function for the background. To

TABLE III: The numbers of candidate events,  $N_{\text{ev}}$ , and values of  $\sin 2\phi_1$  for various subsamples (statistical errors only).

Sample	$N_{\text{ev}}$	$\sin 2\phi_1$
$J/\psi K_S^0(\pi^+\pi^-)$	1116	$0.73 \pm 0.10$
$(c\bar{c})K_S^0$ except $J/\psi K_S^0(\pi^+\pi^-)$	523	$0.67 \pm 0.17$
$J/\psi K_L^0$	1230	$0.78 \pm 0.17$
$J/\psi K^{*0}(K_S^0\pi^0)$	89	$0.04 \pm 0.63$
$f_{\text{tag}} = B^0$ ( $q = +1$ )	1465	$0.65 \pm 0.12$
$f_{\text{tag}} = \bar{B}^0$ ( $q = -1$ )	1493	$0.77 \pm 0.09$
$0 < r \leq 0.5$	1600	$1.27 \pm 0.36$
$0.5 < r \leq 0.75$	658	$0.62 \pm 0.15$
$0.75 < r \leq 1$	700	$0.72 \pm 0.09$
data before 2002	1587	$0.78 \pm 0.10$
data in 2002	1371	$0.65 \pm 0.11$
All	2958	$0.72 \pm 0.07$

account for a small number of events that give large  $\Delta t$  in both the signal and background, we introduce the PDF of the outlier component,  $P_{\text{ol}}$ , and its fraction  $f_{\text{ol}}$ . The only free parameter in the final fit is  $\sin 2\phi_1$ , which is determined by maximizing the likelihood function  $L = \prod_i P_i$ , where the product is over all events. The result of the fit is

$$\sin 2\phi_1 = 0.719 \pm 0.074(\text{stat}) \pm 0.035(\text{syst}).$$

The systematic error is dominated by uncertainties in the vertex reconstruction (0.022). Other significant contributions come from uncertainties in  $w_l$  (0.015), the resolution function parameters (0.014), a possible bias in the  $\sin 2\phi_1$  fit (0.011), and the  $J/\psi K_L^0$  background fraction (0.010). The errors introduced by uncertainties in  $\Delta m_d$  and  $\tau_{B^0}$  are less than 0.010.

Several checks on the measurement are performed. Table III lists the results obtained by applying the same analysis to various subsamples. All values are statistically consistent with each other. Figures 3(a)–3(c) show the raw asymmetries and the fit results for all modes combined,  $(c\bar{c})K_S^0$ , and  $J/\psi K_L^0$ , respectively. A fit to the non- $CP$  eigenstate modes  $B^0 \rightarrow D^{(*)-}\pi^+$ ,  $D^{*-}\rho^+$ ,  $J/\psi K^{*0}(K^+\pi^-)$ , and  $D^{*-}\ell^+\nu$ , where no asymmetry is expected, yields  $0.005 \pm 0.015(\text{stat})$ . Figure 3(d) shows the raw asymmetry for these non- $CP$  control samples.

The signal PDF for a neutral  $B$  meson decaying into a  $CP$  eigenstate [Eq. (2)] can be expressed in a more general form as

$$\mathcal{P}_{\text{sig}}(\Delta t, q, w_l) = \frac{e^{-|\Delta t|/\tau_{B^0}}}{4\tau_{B^0}} \left\{ 1 + q(1 - 2w_l) \left[ \frac{2\text{Im}\lambda}{|\lambda|^2 + 1} \sin(\Delta m_d \Delta t) + \frac{|\lambda|^2 - 1}{|\lambda|^2 + 1} \cos(\Delta m_d \Delta t) \right] \right\}, \quad (4)$$

where  $\lambda$  is a complex parameter that depends on both  $B^0$ - $\bar{B}^0$  mixing and on the amplitudes for  $B^0$  and  $\bar{B}^0$  decay to a  $CP$  eigenstate. The presence of the cosine term ( $|\lambda| \neq 1$ ) would



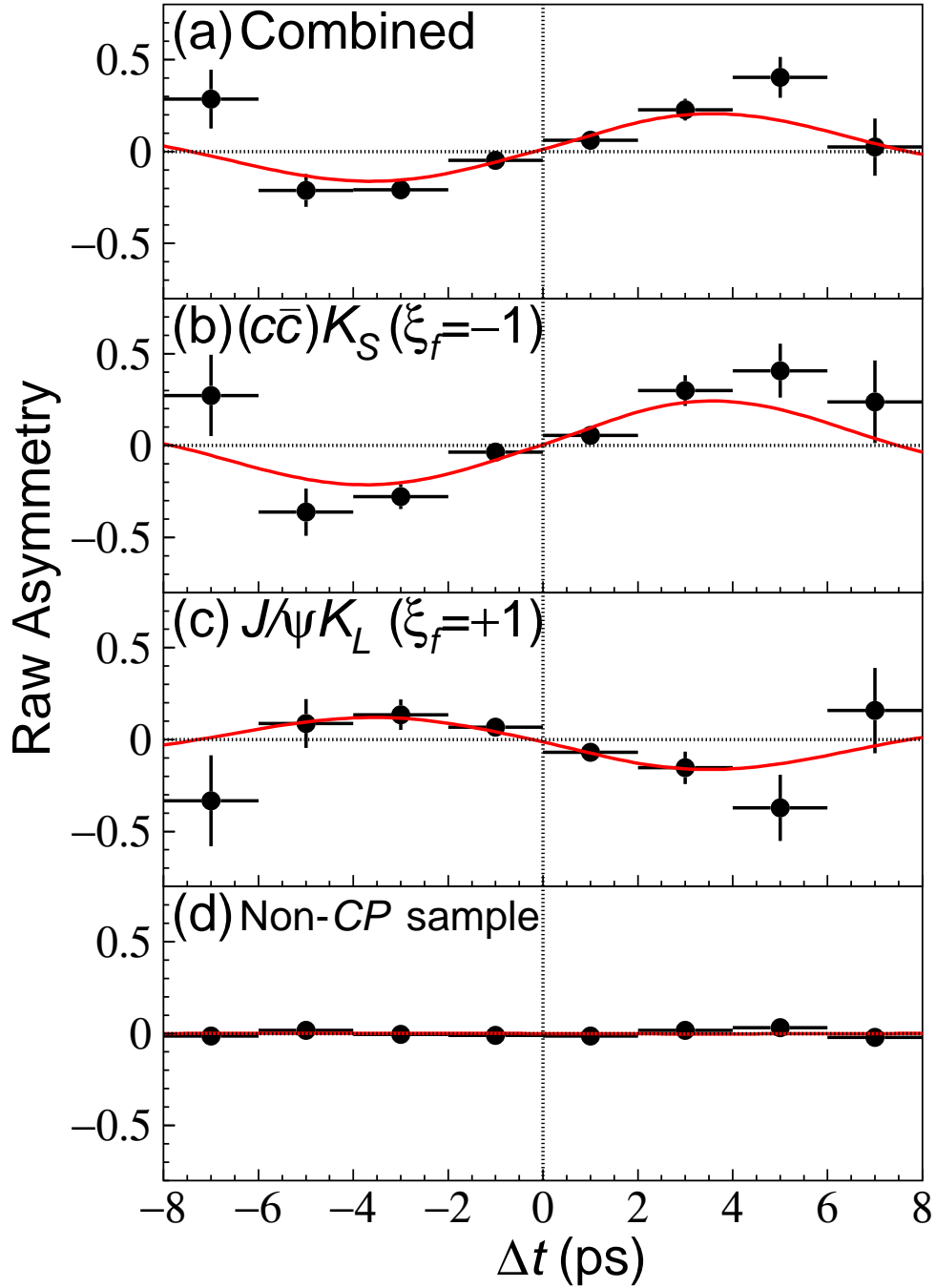


FIG. 3: (a) The raw asymmetry for all modes combined. The asymmetry for  $J/\psi K_L^0$  and  $J/\psi K^{*0}$  is inverted to account for the opposite  $CP$  eigenvalue. The corresponding plots for (b)  $(c\bar{c})K_S^0$ , (c)  $J/\psi K_L^0$ , and (d) non- $CP$  control samples are also shown. The curves are the results of the unbinned maximum likelihood fit applied separately to the individual data samples.

indicate direct  $CP$  violation; the value for  $\sin 2\phi_1$  reported above is determined with the assumption  $|\lambda| = 1$ , as  $|\lambda|$  is expected to be very close to one in the SM. In order to test this assumption, we also performed a fit using the above expression with  $a_{CP} = -\xi_f \text{Im}\lambda/|\lambda|$  and  $|\lambda|$  as free parameters, keeping everything else the same. We obtain

$$|\lambda| = 0.950 \pm 0.049(\text{stat}) \pm 0.025(\text{syst})$$

and  $a_{CP} = 0.720 \pm 0.074(\text{stat})$  for all  $CP$  modes combined, where the sources of the systematic error for  $|\lambda|$  are the same as those for  $\sin 2\phi_1$ . This result is consistent with the assumption used in our analysis.

We wish to thank the KEKB accelerator group for the excellent operation of the KEKB accelerator. We acknowledge support from the Ministry of Education, Culture, Sports, Science, and Technology of Japan and the Japan Society for the Promotion of Science; the Australian Research Council and the Australian Department of Industry, Science and Resources; the National Science Foundation of China under contract No. 10175071; the Department of Science and Technology of India; the BK21 program of the Ministry of Education of Korea and the CHEP SRC program of the Korea Science and Engineering Foundation; the Polish State Committee for Scientific Research under contract No. 2P03B 17017; the Ministry of Science and Technology of the Russian Federation; the Ministry of Education, Science and Sport of the Republic of Slovenia; the National Science Council and the Ministry of Education of Taiwan; and the U.S. Department of Energy.

---

\* on leave from Nova Gorica Polytechnic, Nova Gorica

† on leave from University of Toronto, Toronto ON

- [1] M. Kobayashi and T. Maskawa, *Prog. Theor. Phys.* **49**, 652 (1973).
- [2] A. B. Carter and A. I. Sanda, *Phys. Rev. D* **23**, 1567 (1981); I. I. Bigi and A. I. Sanda, *Nucl. Phys.* **B193**, 85 (1981).
- [3] Belle Collaboration, K. Abe *et al.*, *Phys. Rev. Lett.* **87**, 091802 (2001); *Phys. Rev. D* **66**, 032007 (2002).
- [4] BaBar Collaboration, B. Aubert *et al.*, *Phys. Rev. Lett.* **87**, 091801 (2001); *Phys. Rev. D* **66**, 032003 (2002).
- [5] Belle Collaboration, K. Abe *et al.*, *Phys. Rev. Lett.* **88**, 171801 (2002).
- [6] Belle Collaboration, A. Abashian *et al.*, *Nucl. Instrum. Methods Phys. Res. A* **479**, 117 (2002).
- [7] KEK Report No. 2001-157, edited by E. Kikutani, 2001 [*Nucl. Instrum. Methods Phys. Res. A* (to be published)].
- [8] Throughout this paper, when a decay mode is quoted, the inclusion of the charge conjugate mode is implied.
- [9] Belle Collaboration, K. Abe *et al.*, *Phys. Lett. B* **538**, 11 (2002).
- [10] H. Kakuno *et al.*, (unpublished).
- [11] Particle Data Group, K. Hagiwara *et al.*, *Phys. Rev. D* **66**, 010001 (2002).